# Unified equations of state for neutron stars

Nicolas Chamel
Institute of Astronomy and Astrophysics
Université Libre de Bruxelles, Belgium

INT Seattle, 26 June 2023

# Challenge

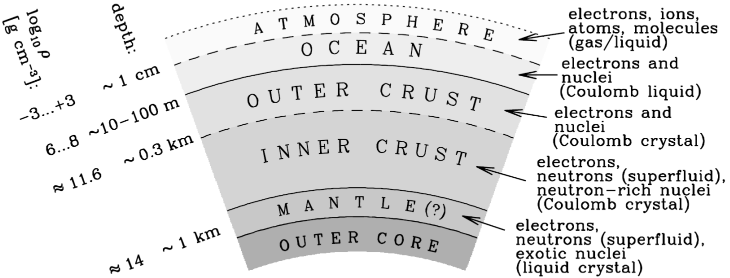


*picture taken from Haensel, Potekhin, Yakovlev, “Neutron Stars” (Springer, 2007)*

- very **different phases** (e.g. gas, liquid, solid, superfluid)
- **huge range of densities** (from $\sim 1$ to $\sim 10^{15}$ g cm$^{-3}$)
- possibly exotic particles (hyperons, quarks) in the inner core.

*Blaschke&Chamel, Astrophys. Space Sci. Lib. 457, eds L. Rezzolla, P. Pizzochero, D. I. Jones, N. Rea, I. Vidaña p. 337-400 (Springer, 2018), arXiv:1803.01836*

# On the importance of a consistent description

Ad hoc matching of different models of dense matter can lead to **significant errors on the neutron-star structure & dynamics**:

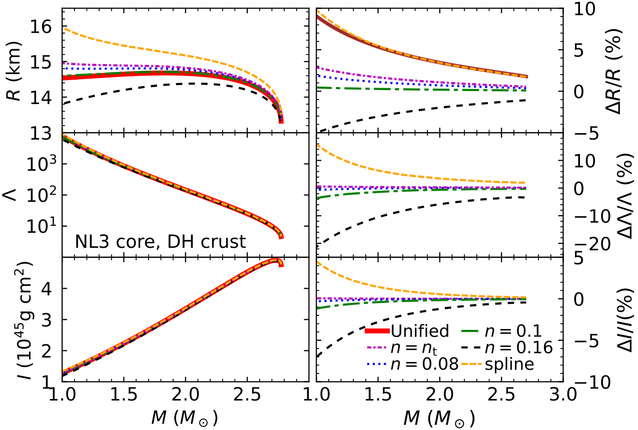


*Suleiman et al., Phys. Rev. C 104, 015801 (2021)*

# Outline

1. Internal constitution of a neutron star
   - Microscopic model of dense matter
   - Constraints from ab initio calculations and laboratory experiments
   - Role of accretion from a stellar companion
   - Role of strong magnetic fields

2. Comparison with astrophysical observations
   - Direct Urca cooling vs observed thermal emission
   - NICER view of PSR J0740+6620
   - Multimessenger observations of GW170817

3. Conclusions & perspectives

# Description of the outer crust of a neutron star

**Traditional approach:** numerical minimization of the Gibbs free energy per nucleon at different pressures $P$ (cold catalyzed matter)
*Tondeur, A&A 14, 451 (1971); Baym, Pethick, Sutherland, ApJ 170, 299 (1971)*

- layers can be easily missed if $\delta P$ not small enough!
- numerically costly (BPS considered 130 even nuclei vs $\sim 10^4$)

**New approach:** iterative minimization of the pressures between adjacent crustal layers (approximate analytical formulas)
*Chamel, Phys. Rev. C 101, 032801(R) (2020)*

- very accurate and reliable ($\delta P/P \sim 10^{-3}$ %)
- composition and stratification (depths, abundances)
- $\sim 10^6$ times faster

Freely available computer code:
`http://doi.org/10.5281/zenodo.3719439`

**Nuclear-physics inputs:** Masses of atomic nuclei

# Experimentally determined layers

- The pressure is mainly given by the electron Fermi gas.
- The composition is completely determined by experimental data down to $\sim$ 200m for a $1.4 M_{\odot}$ neutron star with $R = 10$ km.

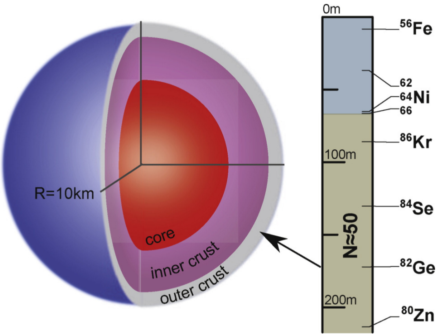


Importance of magic nuclei

But constraints on $Z$ due to beta equilibrium and electric charge neutrality

Few layers with $Z = 28$

**Lack of measurements** of neutron-rich nuclei with $Z \sim 40$ and $N \sim 82$

*Kreim et al., Int.J.M.Spec.349-350,63(2013)*

*Wolf et al.,Phys.Rev.Lett.110,041101(2013)*

Deeper, matter is treated via the **energy density functional theory**.

# Brussels Skyrme functionals (BSk, BSkG)

For application to neutron stars, functionals are fitted to properties of both finite nuclei and infinite homogeneous nuclear matter via self-consistent **Hartree-Fock-Bogoliubov (HFB) calculations**

**Experimental data/constraints**:

- $\sim 2300$ atomic masses (rms $\sim 0.5 - 0.6$ MeV$/c^2$)
- $\sim 900$ nuclear charge radii (rms $\sim 0.03$ fm)
- symmetry energy $29 \leq J \leq 32$ MeV (no good mass fit beyond!)
- incompressibility $K_v = 240 \pm 10$ MeV (giant resonances in nuclei)

**Many-body calculations**:

- equation of state of pure neutron matter
- $^1S_0$ pairing gaps in neutron and symmetric matter
- effective masses in nuclear matter (+giant resonances in nuclei)
- stability against spin and spin-isospin fluctuations

# Neutron-matter constraint

BSk19-21 were simultaneously fitted to three realistic neutron-matter equations of state with different degrees of stiffness:

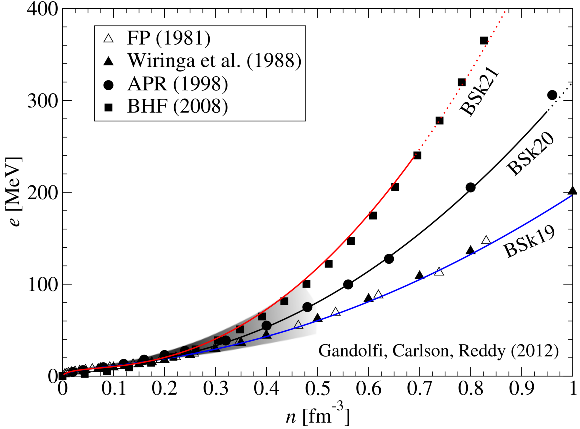


*Goriely, Chamel, Pearson, Phys.Rev.C 82, 035804 (2010)*

# Symmetry-energy constraint

BSk22-26 were adjusted to different values of $J = S(n_0)$. The fit to nuclear masses actually fixes $S(n)$ around $n \sim 0.1$ fm$^{-3}$:

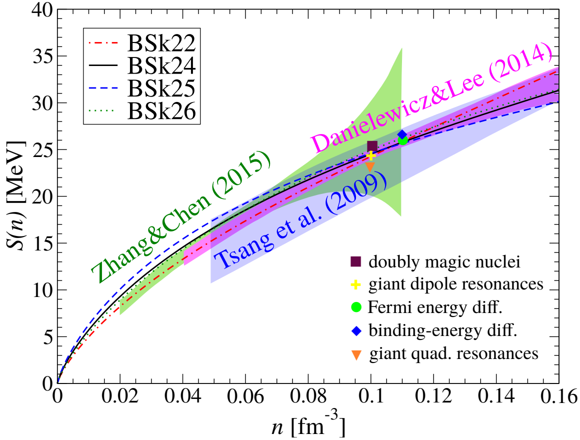


*Goriely, Chamel, Pearson, Phys.Rev.C 88, 024308 (2013)*

# Role of the symmetry energy in the outer crust

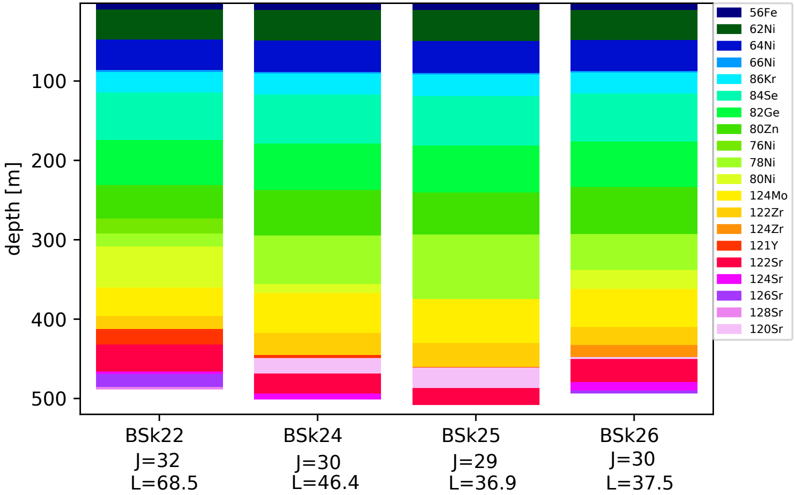


*Structure of a neutron star of mass* $1.5M_\odot$ *and radius 13 km (figure prepared by A. F. Fantina)*

*Pearson et al., MNRAS 481, 2994 (2018)*

# Description of the inner crust of a neutron star

Full HFB calculations are computationally very costly. Intead, we use the **Extended Thomas-Fermi+Strutinsky Integral** (ETFSI) method:

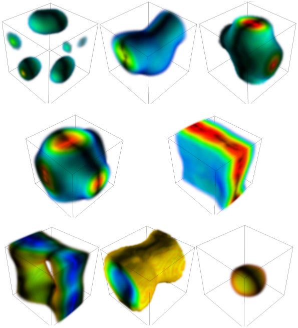

Schuetrumpf et al., PRC87, 055805 (2013)

- **semiclassical expansion up to $\hbar^4$**: the energy reduces to a functional of $n_n(\boldsymbol{r}), n_p(\boldsymbol{r})$ instead of $\Psi_n(\boldsymbol{r}), \Psi_p(\boldsymbol{r})$
- To speed-up the computations, $n_n(\boldsymbol{r}), n_p(\boldsymbol{r})$ are parametrized
- **proton shell effects** are added perturbatively together with **proton BCS pairing**

*Pearson et al., MNRAS 481, 2994 (2018)*

The ETFSI method is a **fairly accurate and computationally very fast** approximation to the full HFB equations

*Shelley&Pastore, Universe 6, 206 (2020)*

# Role of shell effects and symmetry energy

The composition of the inner crust is strongly influenced by the symmetry energy but also by proton shell effects:

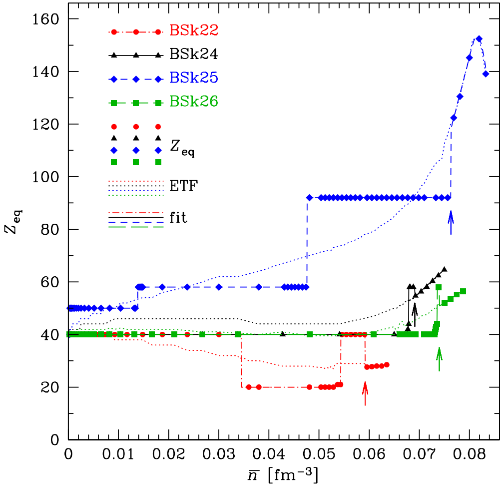


Terrestrial abundances:

Zirconium ($Z = 40$): 0.02%

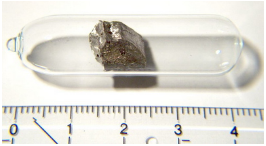


Cerium ($Z = 58$): 0.007%

# Nuclear pastas in neutron stars

According to liquid-drop models, nuclear pastas could represent about **50% of the crust mass.**

e.g. *Newton et al. EpJA58, 69 (2022); Dinh Thi et al., A&A 654, A114 (2021)*

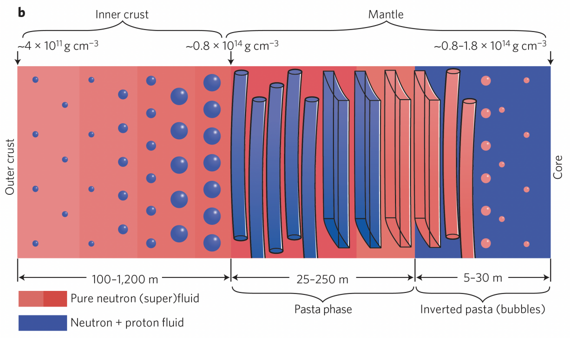


*W. G. Newton, Nature Phys. 9, 396 (2013)*

Pastas could have important implications for the evolution of neutron stars and their gravitational-wave emission.

# Nuclear pastas with ETF(SI) approach

Ignoring SI correction (pure ETF calculations):

- Similar sequence as liquid-drop models
- Negligible impact ($< 1\%$) on the equation of state

*Pearson et al., Phys. Rev. C 101, 015802 (2020)*

# Nuclear pastas with ETF(SI) approach

Ignoring SI correction (pure ETF calculations):

- Similar sequence as liquid-drop models
- Negligible impact ($< 1\%$) on the equation of state

*Pearson et al., Phys. Rev. C 101, 015802 (2020)*

**With SI correction, spaghetti are strongly disfavored**

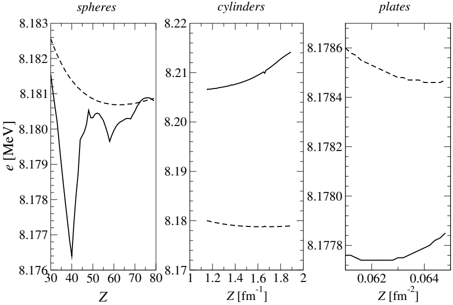


- No true "shell" effects in pastas (smooth fluctuations)
- Origin of SI correction: overbinding of ETF vs HFB, underbinding due to parametrized nucleon profiles

*Pearson&Chamel, Phys. Rev. C 105, 015803 (2022)*

# Nuclear pastas with ETF(SI) approach

The pasta mantle shrinks dramatically in ETFSI!

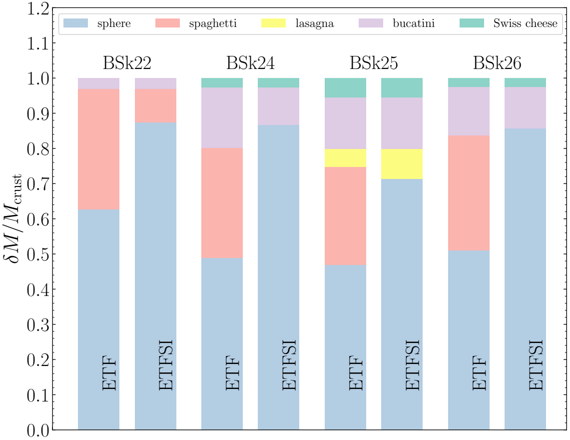


*Shchechilin, Chamel, Pearson, submitted*

# Unified BSk19-26 equations of state

We have constructed **thermodynamically consistent** equations of state for all regions (outer+inner crusts, core) of neutron stars.
*Fantina et al., A&A 559, A128 (2013); Pearson et al.,MNRAS 481, 2994 (2018)*

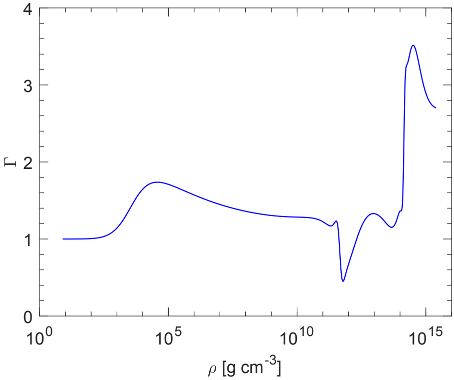


Unified equations of state can hardly be parametrized by polytropes!

$$\Gamma \equiv \left(1 + \frac{P}{\rho c^2}\right) \frac{d \log P}{d \log \rho}$$

# Accretion and X-ray binaries

The composition of the surface layers may be changed by

- the **fallback** of material from the supernova explosion,
- the **accretion** of matter from a stellar companion.

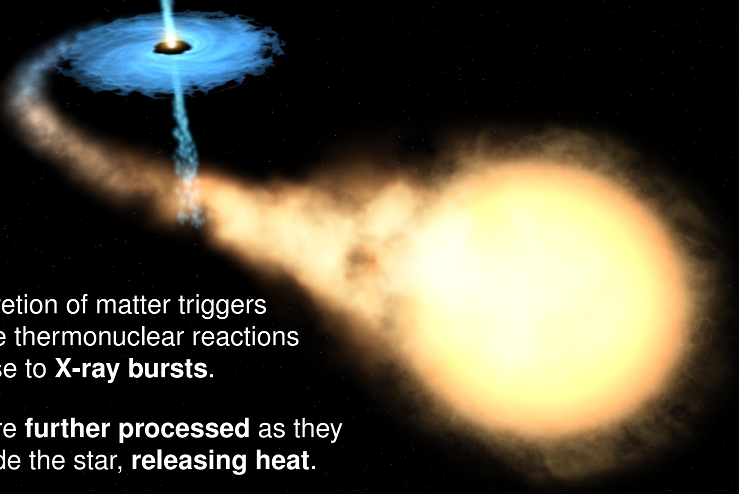

The accretion of matter triggers explosive thermonuclear reactions giving rise to **X-ray bursts.**

Ashes are **further processed** as they sink inside the star, **releasing heat.**

# Composition of accreted crusts and heating

The original crust is buried in the core and replaced by accreted material with very different properties.

Composition and equation of state for ashes made of $^{56}$Fe:

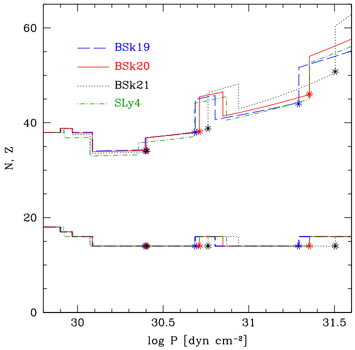


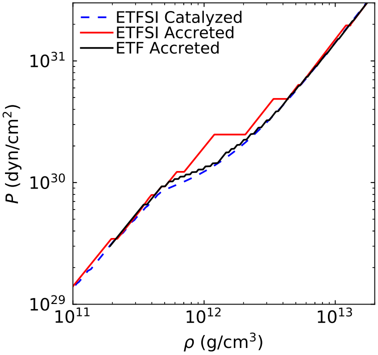


Results are very sensitive to shell effects (magic number $Z = 14$)

*Fantina et al., A&A 620, A105 (2018);A&A 665, A74 (2022)*

# Highly-magnetized neutron stars

Some neutron stars are endowed with **extremely high surface magnetic fields** $\sim 10^{14} - 10^{15}$ G, as inferred from spin-down and spectroscopic studies.

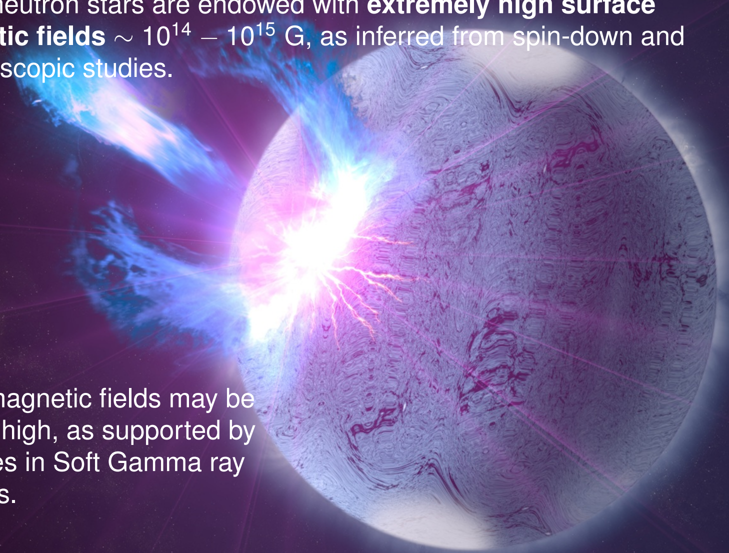

Internal magnetic fields may be also very high, as supported by giant flares in Soft Gamma ray Repeaters.

# Consequence of a high internal magnetic field

In a high magnetic field $\boldsymbol{B}$ (along the $z$-axis), the **electron motion perpendicular to $\boldsymbol{B}$ is quantized into Landau-Rabi levels**

The equation of state and the composition of the crust are altered but the core remains unaffected unless $B \gg 10^{17}$ G.

*Mutafchieva et al., Phys. Rev. C 99, 055805 (2019)*

Freely available computer code for the outer crust:

`http://doi.org/10.5281/zenodo.3839787`

*Chamel&Stoyanov,Phys. Rev. C 101, 065802 (2020)*

The slow magnetic-field decay may further change the composition due to electron captures and pycnonuclear fusions

*Chamel et al., Universe 7(6), 193 (2021)*

*Chamel & Fantina, Universe 8(6), 328 (2022)*

# Direct Urca cooling vs observations

| EoS | $n$ (fm$^{-3}$) | $\rho$ (g cm$^{-3}$) | $M_{\rm DU}/M_{\odot}$ |
|---|---|---|---|
| BSk22 | 0.33 | $5.88 \times 10^{14}$ | 1.15 |
| BSk21/24 | 0.45 | $8.25 \times 10^{14}$ | 1.60 |
| BSk25 | 0.47 | $8.56 \times 10^{14}$ | 1.61 |
| BSk19/20/26 | – | – | – |

The very fast direct Urca cooling process is required to explain

- the thermal luminosities of some accreting neutron stars in quiescence (e.g. SAX J1808.4$-$3658)
  *Yakovlev et al., A&A 417, 169 (2004)*
- the thermal relaxation of some transiently accreting neutron stars (e.g. MXB 1659$-$29).
  *Brown et al.,PRL 120, 182701 (2018)*

- The dUrca process is allowed in all models but BSk19/20/26.
- The low value for $M_{\rm DU}$ predicted by BSk22 implies that dUrca would operate in most neutron stars at variance with observations, but could be suppressed by superfluidity.

# NICER and XMM Newton observations

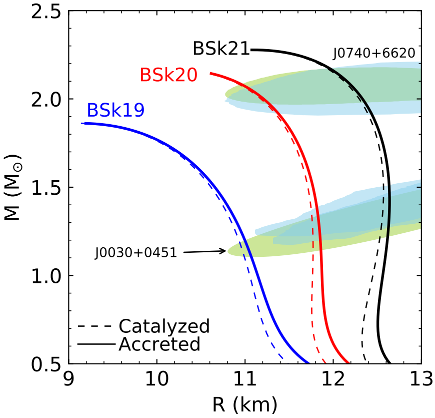


*Fantina et al., A&A 665, A74 (2022)*

- BSk19 is too soft to explain PSR J0740+6620.
- Both accreted and catalyzed models are consistent with observations.

# Gravitational-wave observations

The detection of GW170817 by the LIGO-Virgo collaboration provided the first measurement of the tidal deformability of neutron stars.

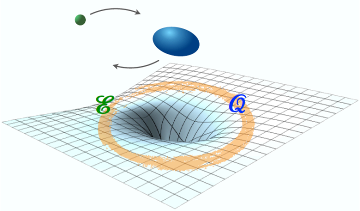


The quadrupolar tidal field $\mathcal{E}_{ij}$ from the companion induces a non-zero quadrupole moment $Q_{ij} \approx \lambda \mathcal{E}_{ij}$

*Dietrich et al., Gen. Relativ. Gravit. 53, 27 (2021)*

$\lambda$ is related to the **Love number** $k_2 = (3/2) G\lambda / R^5$. What was actually extracted from the signal is the **tidal deformability**:

$$\Lambda = \frac{2}{3} k_2 \left( \frac{c^2 R}{GM} \right)^5$$

# Tidal deformability of neutron stars

The tidal deformability coefficient $\Lambda$ of a $1.4M_\odot$ neutron star is strongly correlated with $R$ hence also with the symmetry energy:

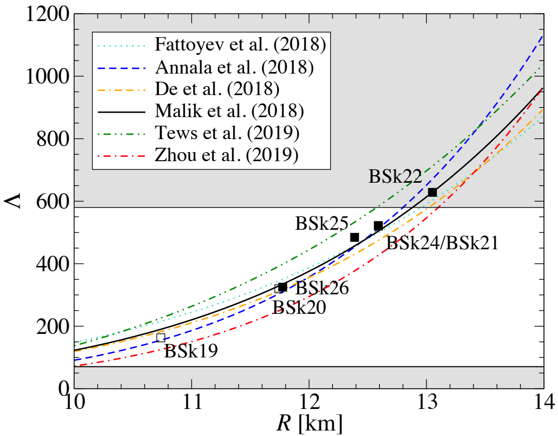


*Perot,Chamel,Sourie,Phys.Rev.C 100, 035801 (2019)*

# Symmetry energy and Love number

The Love number $k_2$ is insensitive to the symmetry energy:

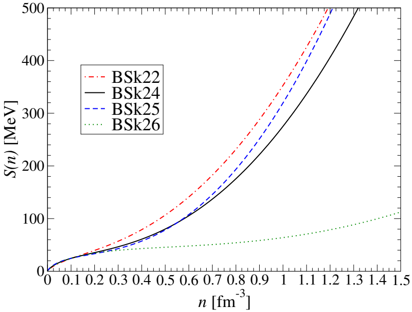


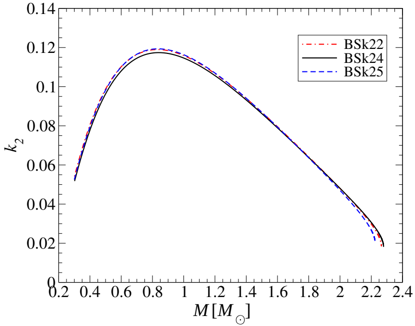


*Perot,Chamel,Sourie,Phys.Rev.C 100, 035801 (2019)*

The dependence of $\Lambda = (2/3)k_2(Rc^2/GM)^5$ on the symmetry energy thus arises mainly from the factor $R^5$.

# Neutron matter and Love number

The Love number is mostly governed by the neutron-matter stiffness: the softer the equation of state, the lower $k_2$ is.

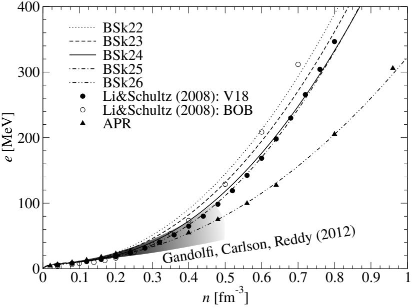


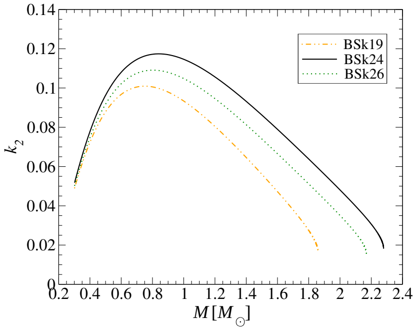


*Perot,Chamel,Sourie,Phys.Rev.C 100, 035801 (2019)*

Full results for tidal coefficients up to $\ell = 5$:

*Perot&Chamel, Phys.Rev.C103, 025801 (2021)*

# Role of the “crust” on the tidal deformability

**Different approaches with different conclusions:**

*Piekarewicz&Fattoyev*
*Phys.Rev.C99,045802 (2019)*

- BPS for the outer crust (using Duflo&Zuker mass table)
- RMF (FSUGarnet) for the core
- polytropes for the inner crust

$\delta\Lambda_{1.4}/\Lambda_{1.4} \lesssim 0.1\%$ when varying the polytropic index

*Kalaitzis, Motta, Thomas*
*Int.J.Mod.Phys. E28,1950081 (2019)*

tabulated EoSs fitted using two polytropes for the core

$\delta\Lambda_{1.4}/\Lambda_{1.4} \lesssim 10\%$ when comparing to fitted EoS extrapolated to lower densities

*Ji et al., Phys.Rev.C100, 045801(2019)*

$\delta\Lambda_{1.4}/\Lambda_{1.4} \sim 3\%$ when matching different crusts to the same core

# Role of the "crust" on the tidal deformability

Comparison with purely homogeneous neutron stars for BSk24:

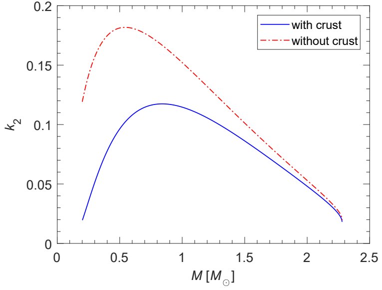


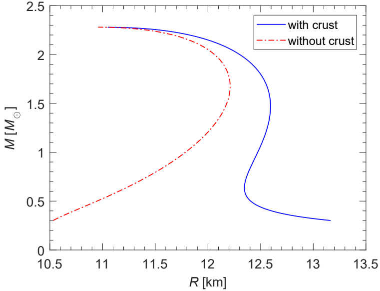


*Perot et al.,Phys.Rev.C101, 015806 (2020)*

- Changes in $k_2$ are essentially due to $\Delta R$ ($\Rightarrow$ analytic formula)
- Changes in $\Lambda \propto k_2 R^5$ are small ($< 1\%$): the strong reduction of $k_2$ is compensated by the increase of $R$

The crust may still lead to $\sim 1\%$ systematic errors on the radii inferred from the analysis of the gravitational-wave signal

*Gamba et al., Class. Quantum Grav. 37, 025008 (2020)*

# Measurements of tidal deformabilities

The tidal deformabilities extracted from the analysis of GW170817 disfavor a stiff symmetry energy (BSk22):

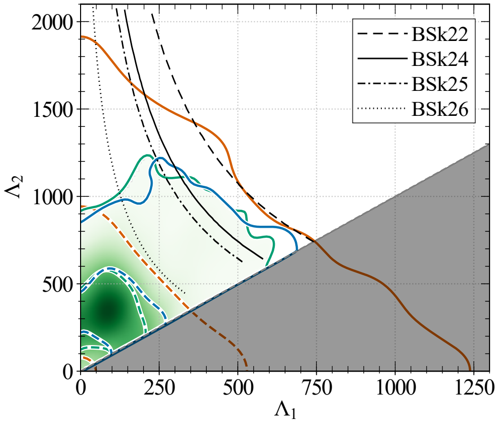


*Perot,Chamel,Sourie,Phys.Rev.C 100, 035801 (2019)*

# LIGO-Virgo observations of GW170817

The gravitational-wave data alone tend to favor a **soft EoS at intermediate densities** (BSk19), as supported by $K^+$ production and $\pi^-/\pi^+$ production ratio in heavy-ion collisions

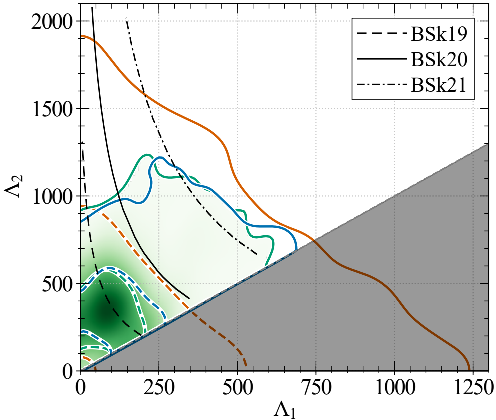


*Perot,Chamel,Sourie,Phys.Rev.C 100, 035801 (2019)*

# Constraints from electromagnetic counterparts

The ejected mass $\sim 0.02 - 0.05 M_{\odot}$ inferred from electromagnetic observations suggests a delayed collapse:

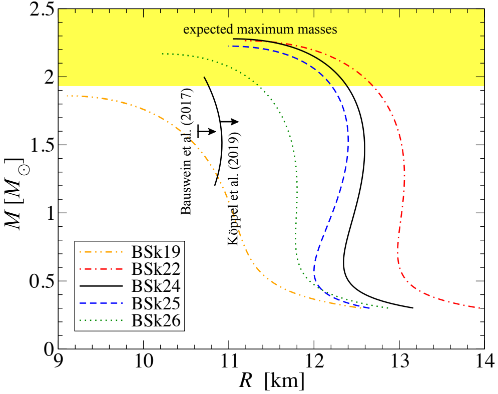


*Perot,Chamel,Sourie,Phys.Rev.C 100, 035801 (2019)*

Electromagnetic observations favor a stiff EoS at high densities.

# Conclusions & Perspectives

We have constructed **thermodynamically consistent equations of state for isolated, accreted and highly magnetized neutron stars** based on precision-fitted nuclear functionals

Tables available on CompOSE: `https://compose.obspm.fr/`

Freely available computer codes and data for the outer crust:
`http://doi.org/10.5281/zenodo.3719439`
`http://doi.org/10.5281/zenodo.3839787`

Consistent ${}^1S_0$ pairing gaps: *Allard&Chamel, Universe 7(12), 470 (2021)*

Ongoing:

- New functionals based on full 3D HFB (G. Grams, W. Ryssens)
- Full 3D HFB calculations of nuclear pastas (N. Schechilin)
- Extension to finite temperatures (C. Mondal)

# Addendum: nuclear-matter parameters

| | BSk22 | BSk23 | BSk24 | BSk25 | BSk26 |
|---|---|---|---|---|---|
| $a_v$ [MeV] | -16.088 | -16.068 | -16.048 | -16.032 | -16.064 |
| $n_0$ [fm$^{-3}$] | 0.1578 | 0.1578 | 0.1578 | 0.1587 | 0.1589 |
| $J$ [MeV] | 32.0 | 31.0 | 30.0 | 29.0 | 30.0 |
| $L$ [MeV] | 68.5 | 57.8 | 46.4 | 36.9 | 37.5 |
| $K_{sym}$[MeV] | 13.0 | -11.3 | -37.6 | -28.5 | -135.6 |
| $K_v$ [MeV] | 245.9 | 245.7 | 245.5 | 236.0 | 240.8 |
| $K'$ [MeV] | 275.5 | 275.0 | 274.5 | 316.5 | 282.9 |
| $M_s^*/M$ | 0.80 | 0.80 | 0.80 | 0.80 | 0.80 |
| $M_v^*/M$ | 0.71 | 0.71 | 0.71 | 0.74 | 0.65 |

Lower and higher values of $J$ were considered but yielded substantially worse fits to atomic masses.

*Goriely, Chamel, Pearson, Phys.Rev.C 88, 024308 (2013).*